2010

Adaptive Optical splitter Employing an Opto-VLSI Processor and a 4-f Imaging System

Haithem AB Mustafa
Edith Cowan University

Feng Xiao
Edith Cowan University

Kamal Alameh
Edith Cowan University

10.1109/JLT.2010.2062487
This article was originally published as: Mustafa, H. A., Xiao, F., & Alameh, K. (2010). Adaptive Optical splitter Employing an Opto-VLSI Processor and a 4-f Imaging System. Journal of Lightwave Technology, 28(19), 2761-2765. Original article available here

Adaptive Optical Splitter Employing an Opto-VLSI Processor and a 4-f Imaging System

Haithem A. B. Mustafa, Feng Xiao, and Kamal Alameh

***Abstract*—A novel adaptive optical splitter structure employing an Opto-VLSI processor and 4-f imaging system is proposed and experimentally demonstrated. By driving the Opto-VLSI processor with computer generated multicasting phase holograms, an input optical signal launched into an input optical fiber port can be split and coupled into many output optical fiber ports with arbitrary splitting ratios. A proof-of-principle 1×2 adaptive optical splitter structure driven by optimized multicasting phase holograms uploaded onto the Opto-VLSI processor is developed, demonstrating an arbitrary splitting ratio over a wavelength range exceeding 50 nm.**

***Index Terms*—Adaptive optical splitter, beam splitter, liquid crystal devices, optical communication, opto-VLSI processor.**

I. Introduction

THE demand for optical power splitters is growing globally, due to the rapid deployment of fiber-to-the-premises (FTTP), optical metropolitan area network (MAN), and active optical cables for TV/Video signal transport [1]. Passive optical network (PON) technology enables several hundred users to share one optical line terminal (OLT) at the central office distributing optical power to several tens of optical network units (ONUs) at the customer end of the network, each of which is shared by many users [2]. However, current PONs, which use fixed optical power splitters, have limited reconfigurability not only to adding/dropping users to/from an ONU but also to changing services for each user. An adaptive optical power splitter can dynamically reallocate the optical power in the entire network according to the real-time distribution of users and services, thus providing numerous advantages such as improvement of optical network efficiency and network scalability, and high network reliability. An adaptive optical power splitter is also necessary for implementing a self-healing ring in a MAN [3], which offers a popular protection mode that automatically recovers communication from failure. Furthermore, future optical line protection (OLP) systems require adaptive optical splitters to: i) transfer the optical power from the primary path to the secondary path dynamically; ii) avoid the use of optical power attenuators and optical amplifiers; and iii) monitor both paths instantaneously [4]. Moreover, adaptive optical power splitters can add many advantages into fiber CATV networks, including substantial improvement in network adaptability and scalability [5].

Currently, the majority of optical power splitters are passive [6]–[10]. Passive splitters based on Planar Lightwave Circuits (PLC) are low-cost, however, they do not provide network flexibility. Recently, only a few dynamic optical splitter structures have been reported. A simple dynamic optical splitter structure has been realized by incorporating an optical amplifier into each output port of a passive splitter [11], [12]. However, such a structure is very expensive and has fundamental limitations, namely, high output noise levels generated by the individual optical amplifiers, and the difficulty in controlling the output power level, since the optical amplifier gain depends on the power level of the split optical signal. Recently, an adaptive optical power splitter structure based on the use of a half wave plate and optical polarization components has been demonstrated [5], where an arbitrary optical splitting ratio is realized by mechanically rotating the half wave plate. The main disadvantages of this splitter structure are: i) limited reliability due to the wear and tear of the mechanically rotated wave plate and ii) the inability to independently control the split output power levels. An adaptive optical splitter employing thermally-tuned fiber Bragg gratings (FBGs) has also been reported [13]. This structure is impractical, due to its high packaging cost and limited tolerance to environmental perturbations (temperature, vibrations, etc). In addition, a 1×3 dynamic optical splitter using an Opto-VLSI processor in conjunction with custom-made piecewise linear optics has been reported [14]. However, this splitter architecture requires custom-made piecewise linear optics integrated with a fiber collimator array, making its mass production very difficult, especially when the number of output ports is large.

In this paper, we propose and experimentally demonstrate the concept of a new adaptive optical splitter structure based on the use of an Opto-VLSI processor in conjunction with a 4-f imaging system. This adaptive optical splitter can be reconfigured via software to provide arbitrary optical power splitting ratios for multiple output channels. In addition, the adaptive splitter has attractive features, such as a simple architecture, ability to synthesize arbitrary and accurate splitting ratios, low power loss, and easy user interface.

II. Opto-VLSI Processors and Optical Beam Multicasting

The Opto-VLSI processor is a diffraction element capable of steering/shaping an incident optical beam electronically without mechanically moving parts. As shown in Fig. 1, an

Manuscript received May 19, 2010; revised July 18, 2010; accepted July 20, 2010. Date of publication August 03, 2010; date of current version September 08, 2010. This work was supported by the State Key Laboratory of Advanced Optical Communication Systems and Networks, China.

The authors are with the Centre of Excellence for MicroPhotonic Systems, Electron Science Research Institute, Edith Cowan University, Joondalup, WA 6027, Australia (e-mail: hmustafa@our.ecu.edu.au).

Color versions of one or more of the figures in this paper are available online at http://ieeexplore.ieee.org.

Digital Object Identifier 10.1109/JLT.2010.2062487

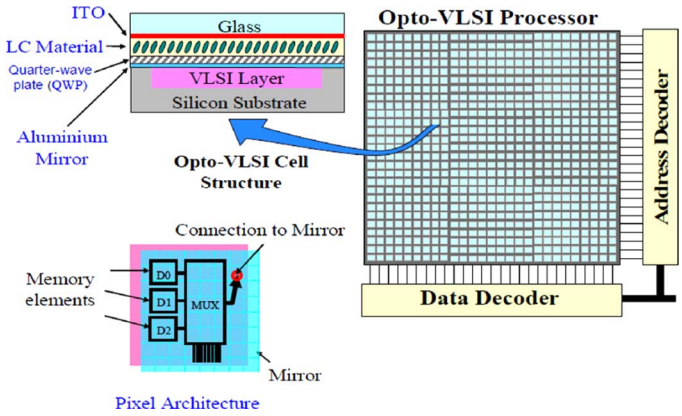

Fig. 1. Opto-VLSI processor layout, Opto-VLSI cell structure and pixel architecture.

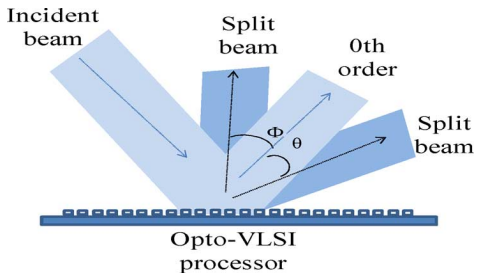

Fig. 2. Illustration of the optical beam multicasting capability of an Opto-VLSI processor.

Opto-VLSI processor comprises an array of liquid crystal (LC) cells driven by a Very-Large-Scale-Integrated (VLSI) circuit [14], [15], which generates digital holographic diffraction gratings that achieve arbitrary beam deflection/multicasting. A transparent Indium-Tin Oxide (ITO) layer is used as the second electrode, and a quarter-wave-plate (QWP) layer is deposited between the *LC* and the aluminum mirror to accomplish polarization-insensitive operation. The voltage level of each pixel can individually be controlled by using a few memory elements that select a discrete voltage level and apply it, through the electrodes, across the *LC* cell.

A multicasting phase hologram can split an incident optical beam to N output beams with variable intensities in different directions, as illustrated in Fig. 2. A collimated beam incident onto the Opto-VLSI processor is diffracted along different directions, where the power of each diffracted beam depends on the multicasting phase hologram. The beam multicasting resolution, or minimum splitting angle relative to the zeroth order diffraction beam, is given by [16]

$$\alpha = \arcsin\left(\frac{\lambda}{N \times d}\right) \tag{1}$$

where λ is the optical wavelength, N denotes the number of pixels illuminated by the incident optical beam, and d is the pixel pitch.

Several computer algorithms, such as the genetic, simulated annealing, phase encoding, and projection algorithms [17], have been used for generating optimized multicasting phase holograms that produce a target far-field distribution, defined by the replay beam positions and the corresponding power splitting ratios. For a target splitting ratio profile, an optimised phase hologram can always be generated, which minimizes the zeroth order diffraction and maximizes the signal-to-crosstalk ratio at every output port.

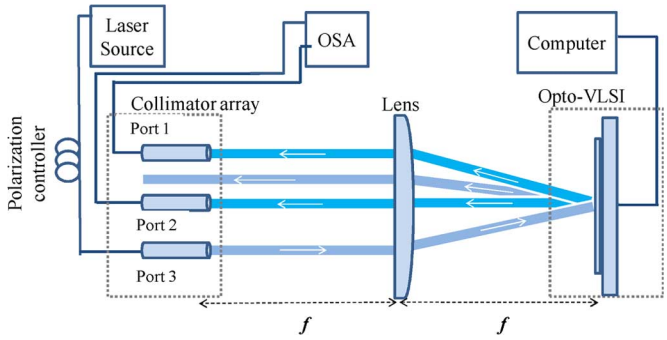

Fig. 3. Schematic diagram of the proposed adaptive optical splitter using an Opto-VLSI processor and a 4-f imaging systems.

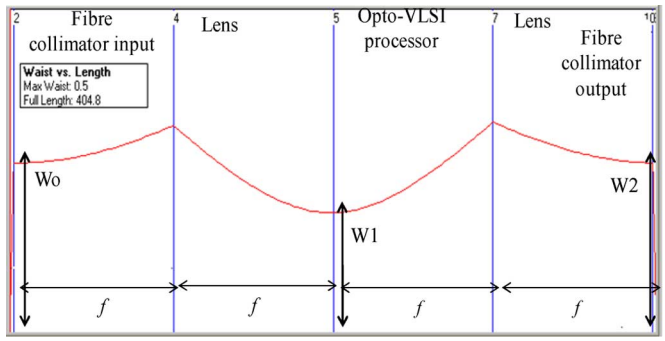

Fig. 4. Simulation results showing the optical beam waist along the 4-f imaging system. W0 is the input beam waist at the input fiber collimator, W1 is the beam waist at the Opto-VLSI processor, and W2 is the waist of the reflected beam as it reaches the output fiber collimator.

III. Experiments

A. System Description

The structure of the proposed adaptive optical power splitter is shown in Fig. 3, through an experimental setup. It consists of an Opto-VLSI processor, a lens, and an optical fiber collimator array, aligned to form a 4-f imaging system. The Opto-VLSI processor has 1×4096 pixels with pixel size of 1.0 μm wide and 6.0 mm length, and 1.8 μm pixel pitch (i.e., 0.8 μm of dead space between pixels). To prove the concept of adaptive optical splitting, only three ports of the fiber collimator were used, thus demonstrating a 1×2 adaptive optical power splitter. A 1550 nm laser source of $+5$ dBm optical power was used as an input signal, and launched through Port 3 of the fiber collimator array. Port 1 and Port 2 were used as the output ports. The spacing (D)between the fiber collimator elements was 3 mm. A lens of focal length $f = 100$ mm was placed between and at an equal distance, f, from both the fiber collimator array and the Opto-VLSI processor. With no phase hologram uploaded onto the Opto-VLSI processor, only the 0th order diffraction beam was reflected back and focused through the imaging system onto a spot in between the fiber collimator ports, resulting in

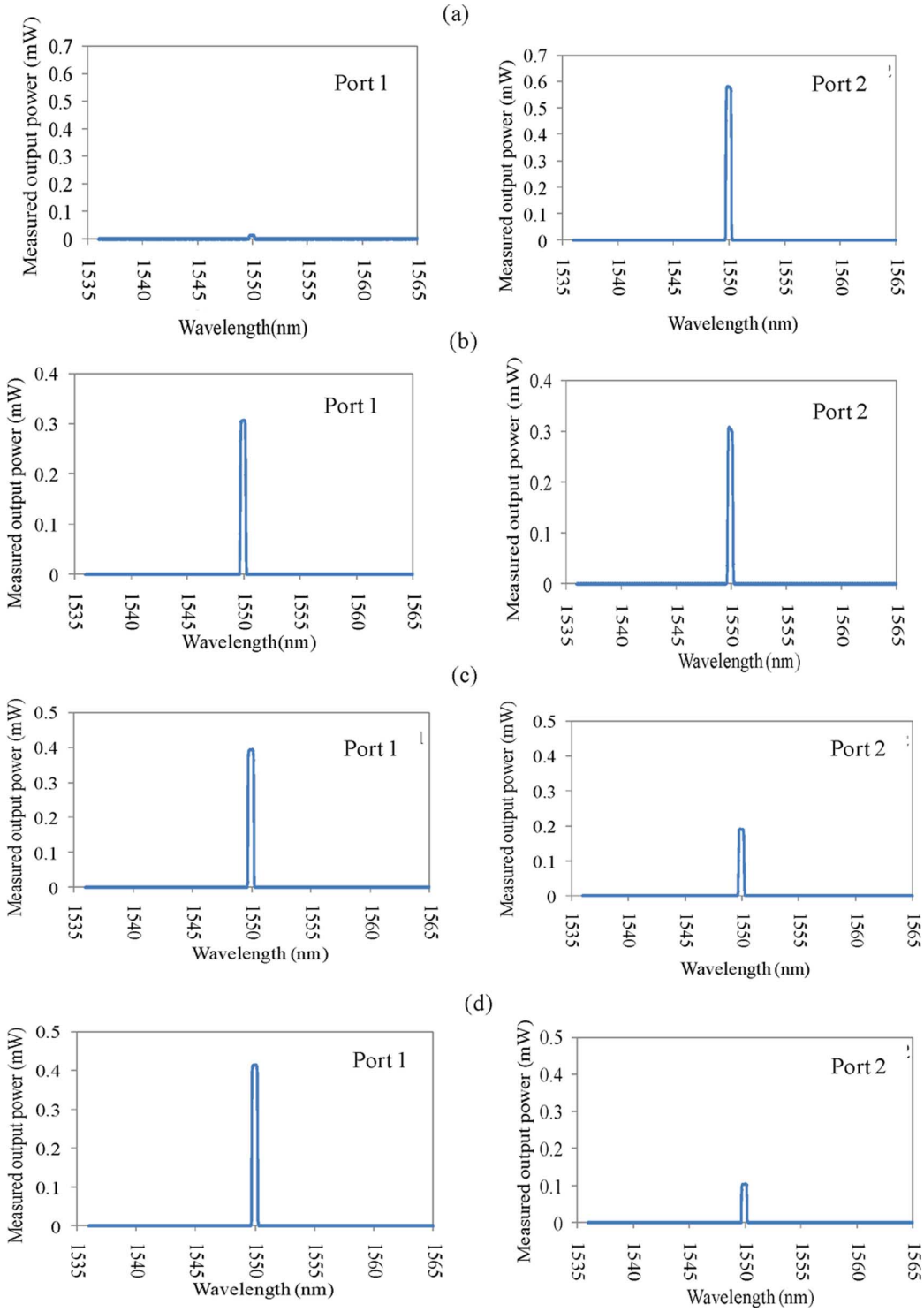

Fig. 5. Measured output power at Port 1 and Port 2 (i.e., P_1 and P_2) for different splitting ratios. (a) Splitting ratio $P_1/P_2 = 0$, (b) $P_1/P_2 = 1$, (c) $P_1/P_2 = 2$, and (d) $P_1/P_2 = 4$.

minimum crosstalk coupled into ports 1 and 2, as illustrated in Fig. 3. Fig. 4 shows the beam waist profile as it propagated through the 4-f imaging system. The beam diameter at the fiber collimator was 0.5 mm, then expanded to 0.72 mm at the lens, which focused it to 0.4 mm at the Opto-VLSI processor. Upon reflection off the Opto-VLSI processor, the beam diameter expanded to 0.72 mm at the lens and reduced to around 0.5 mm at the fiber collimator, then coupled, through the lens of the fiber collimator, into the output fiber ports.

By driving the Opto-VLSI processor with an optimized multicasting phase hologram, the optical beam illuminating the Opto-VLSI processor was split into two different optical beams (in addition to the 0th order beam) which propagated along the optimized directions so that they were respectively coupled back

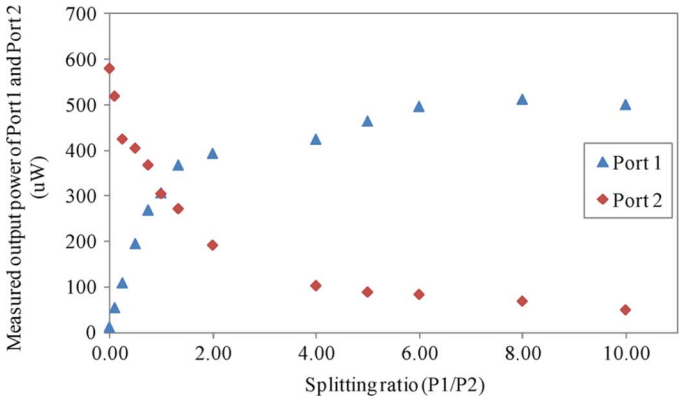

Fig. 6. Measured output powers at Port1 (▲) and Port 2 (♦) versus the splitting ratio (P_1/P_2).

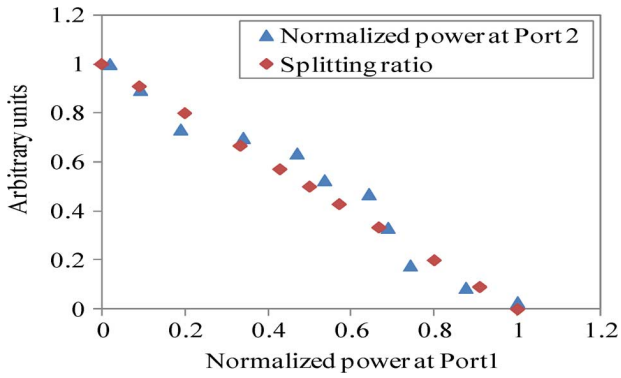

Fig. 7. Normalized output power at Port 2 (▲) and the corresponding splitting ratio (arbitrary units) (♦) versus the normalized power at Port 1.

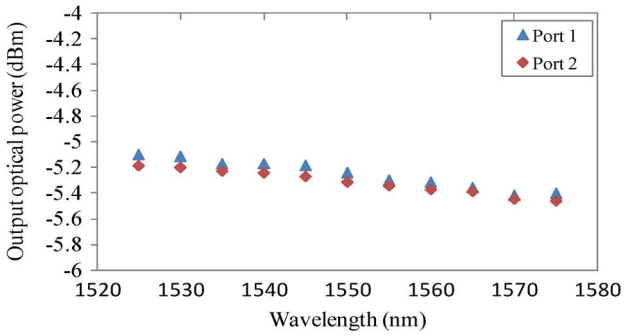

Fig. 8. Measured output power at ports 1 and 2 versus wavelength for a splitting ratio = 1.0.

into Port 1 and 2 of the fiber collimator through the 4-f imaging system. The split optical beams coupled into the two output ports propagated along angles equal to $\theta = \pm\arctan(D/2f) \approx \pm 0.86°$ with respect to the 0th order beam. Two optical spectrum analyzers (OSA) were used to monitor the split signals coupled into the two output ports.

Note that a fiber collimator array, rather than a fiber array, was used in this experiment to avoid stringent alignment conditions, such as the use of highly accurate optical stages, to maximize the optical power coupled into the output ports. Note also that the diameter of the focused optical beam at the Opto-VLSI processor was relatively large, in order to illuminate a large number of pixels, leading to a high diffraction efficiency and high splitting resolution as described in (1). This 4-f imaging system enabled adaptive optical splitting with large tolerance to misalignment to be achieved.

B. Experimental Results and Discussion

Several splitting ratios were attempted to demonstrate the adaptive power splitting capability of the proposed optical splitter. Fig. 5 shows the measured output powers, P_1 and P_2, at Port 1 and Port 2, respectively, corresponding to different splitting ratios.

For a splitting ratio equal to zero (i.e., $P_1 = 0$), as shown Fig. 5(a), the input signal was steered to Port 2, through a steering phase hologram, resulting in a very small signal power being measured at Port 1. The splitting ratio can continuously be changed from 0.021 (−16.6 dB) to around 50 (17 dB). When the splitting ratio changed to 1.0 (i.e., splitting the input power equally to the two output ports), the measured output powers at Port 1 and Port 2 were 307 μW and 305 μW, respectively, as illustrated in Fig. 5(b). Figs. 5(c) and (d) show the output powers at Port 1 and Port 2 when the splitting ratios were set to 2 and 4, respectively. Excellent agreements between the measured power values at the two output ports and the splitting ratios are displayed in Fig. 5.

Fig. 6 shows the measured optical power levels at the two output fiber ports versus the splitting ratio, and demonstrates the ability of the adaptive splitter structure to realize arbitrary splitting ratios.

Fig. 7 shows the measured normalized power at Port 2 $(P_2/P_{tot}$, where $P_{tot} = P_1 + P_2)$ as well as the simulated splitting ratio versus the normalized power at Port 1 (P_1/P_{tot}). It is noticed that the sum of the power levels at the two output ports is constant, demonstrating that the total output power split into Port 1 and Port 2 remains invariable every time a new optimized multicasting phase hologram is uploaded for realizing a target splitting ratio. Fig. 7 demonstrates that the output power can be arbitrarily split between the two output ports.

To investigate the bandwidth of the proposed adaptive optical splitter, a tunable laser source of wavelength range from 1525 nm to 1575 nm was used at the input fiber port. The measured output power at ports 1 and 2 versus wavelength are shown in Fig. 8, for a splitting ratio equal to 1.0. The measured maximum output power fluctuations at the two output ports was less than 0.1 dB over a wavelength span from 1525 to 1575 nm, demonstrating a splitter bandwidth in excess of 50 nm.

The total insertion loss of the optical power splitter was about 5 dB, to which the Opto-VLSI processor contributed around 3 dB due to its low fill factor. The beam steering loss was 0.5 dB and the fiber collimator array in conjunction with the lens contributed the remaining 1.5 dB of insertion loss. However, the total insertion loss can be reduced through (i) an improved Opto-VLSI chip design, where the dead-space between pixels is reduced, and (ii) the use of broadband AR coatings for the various optical components.

The total insertion loss was relatively large for a 1×2 optical splitter. However, this adaptive optical power splitter structure has the potential to realize a large number of output ports with negligible insertion loss penalty. The latter feature makes the

proposed splitter attractive for many emerging optical network applications, in comparison to other adaptive optical power splitters that have a limited number of output ports.

Note that the large port spacing of the collimator array used in this experiment limited the number of output ports. However, by reducing the spacing between the fiber collimator elements to around 1 mm, more than 10 output ports can be achieved. Furthermore, by using a 2-D Opto-VLSI processor and a 2-D fiber collimator array, a high resolution dynamic optical splitter with up to 100 output ports can potentially be realized.

IV. Conclusion

The concept of an adaptive optical splitter employing a 4-f imaging system and an Opto-VLSI processor has been demonstrated for the first time. Experimental results have demonstrated that an input optical signal can arbitrarily be split into two signals and coupled into optical fiber ports by uploading optimized multicasting phase holograms onto the Opto-VLSI processor. A bandwidth exceeding 50 nm over the C-band of optical telecommunications has been measured, making the adaptive splitter attractive for many optical network applications. This proof-of-concept 1×2 adaptive splitting demonstrator opens the way towards the realization of software-driven large-scale adaptive optical power splitters for numerous dynamic optical network applications.

References

[1] G. A. Queller, "Dynamic power distribution in PON/FTTP networks," *Lightwave* vol. 21, no. 7, 2004 [Online]. Available: http://www.lightwaveonline.com/about-us/lightwave-issue-archives/issue/dynamic-power-distribution-in-ponfttp-networks-53906787.html

[2] M. D. Vaughn, D. Kozischek, D. Meis, A. Boskovic, and R. E. Wagner, "Value of reach-and-split ratio increase in FTTH access networks," *J. Lightw. Technol.*, vol. 22, no. 11, pp. 2617–2622, Nov. 2004.

[3] J. Shi and J. P. Fonseka, "Hierarchical self-healing rings," *IEEE/ACM Trans. Netw.*, vol. 3, no. 6, pp. 690–697, Dec. 1995.

[4] D. Griffith and S. Lee, "A 1 + 1 protection architecture for optical burst switched networks," *IEEE J. Sel. Areas Commun.*, vol. 21, no. 9, pp. 1384–1398, Nov. 2003.

[5] Z. Yun, L. Wen, C. Long, L. Yong, and X. Qingming, "A 1×2 variable optical splitter development," *J. Lightw. Technol.*, vol. 24, no. 3, pp. 1566–1570, Mar. 2006.

[6] T. J. Wang, C. F. Huang, and W. S. Wang, "Wide-angle 1×3 optical power divider in LiNbO3 for variable power splitting," *IEEE Photon. Technol. Lett.*, vol. 15, no. 10, pp. 1401–1403, Oct. 2003.

[7] K. B. Chung and J. S. Yoon, "Properties of a 1×4 optical power splitter made of photonic crystal waveguides," *Opt. Quantum Electron.*, vol. 35, pp. 959–966, 2003.

[8] A. Ghaffari, M. Djavid, and M. S. Abrishmian, "Power splitters with different output power levels based on directional coupling," *Appl. Opt.*, vol. 48, no. 8, pp. 1606–1609, 2009.

[9] I. Park, H. S. Lee, H. J. Kim, K. M. Moon, S. G. Lee, B. H. O, S. G. Park, and E. H. Lee, "Photonics crystal power-splitter based on directional coupling," *Opt. Exp.*, vol. 12, no. 15, pp. 3599–3604, 2004.

[10] Y. Zhang, L. Liu, X. Wu, and L. Xu, "Splitting-on-demand optical power splitters using multimode interference (MMI) waveguide with programmed modulations," *Opt. Commun.*, vol. 281, pp. 426–432, 2008.

[11] F. Ratovelomanana, N. Vodjdani, A. Enard, G. Glasere, D. Rondi, and R. Blondeau, "Active lossless monolithic one-by-four splitters/combiners using optical gates on InP," *IEEE Photon. Technol. Lett.*, vol. 7, no. 5, pp. 511–513, May 1995.

[12] S. S. Choi, J. P. Donnelly, S. H. Groves, R. E. Reeder, R. J. Bailey, P. J. Taylor, A. Napoleone, and W. D. Goodhue, "All-active InGaAsP-InP optical tapered-amplifier $1 \times N$ power splitters," *IEEE Photon. Technol. Lett.*, vol. 12, no. 8, pp. 974–976, Aug. 2000.

[13] X. Zhao and S. Jose, "Dynamic Power Optical Splitter," U.S. Patent 7 068 939 B2, Jun. 27, 2006.

[14] R. Zheng, Z. Wang, K. E. Alameh, and W. A. Crossland, "An opto-VLSI reconfigurable broadband optical splitter," *IEEE Photon. Technol. Lett.*, vol. 17, no. 2, pp. 339–341, Feb. 2000.

[15] F. Xiao, B. Juswardy, and K. Alameh, "Novel broadband reconfigurable optical add-drop multiplexer employing custom fiber arrays and opto-VLSI processors," *Opt. Exp.*, vol. 16, no. 16, pp. 11703–11708, 2008.

[16] F. Xiao, K. Alameh, and T. T. Lee, "Opto-VLSI-based tunable single-mode fiber," *Opt. Exp.*, vol. 17, no. 21, pp. 18676–18680, 2009.

[17] S. T. Ahderom, M. Raisi, K. Alameh, and K. Eshraghian, "Testing and analysis of computer generated holograms for microphotonics devices," in *Proc. 2nd IEEE Int. Workshop Electron. Design, Test Appl. (DELTA)*, Australia, 2004, pp. 47–52.

Haithem A. B. Mustafa received the B.Sc. degree in physics and mathematics from the University of Khartoum, Khartoum, Sudan, in 2002, the B.Tech. and M.Tech. degrees in electrical engineering from the Cape Peninsula University of Technology (CPUT), Cape Town, South Africa, in 2005 and 2007, respectively, and the M.S. degree in MEMS and NEMS from the University of Trento, Trento, Italy, in 2008. He is currently working toward the Ph.D. degree at the Electron Science Research Institute, Edith Cowan University, Joondalup, Australia.

Feng Xiao received the Ph.D. degree in electrical engineering from Peking University, Beijing, China, in 2007.

Since November 2007, he has been a Research Fellow with Edith Cowan University, Joondalup, Australia. He has authored or coauthored over 40 papers in refereed journal and conference papers. His current research interests include fiber optics, integrated optics, optical devices, photonic microwave, and photonic signal processing.

Kamal Alameh received the B.Eng.Sc. degree in communications and electronics engineering from the Beirut Arab University, Lebanon, in 1985, the M.Eng. degree in photonics from the University of Melbourne, Melbourne, Australia, in 1989, and the Ph.D. degree in photonics from the University of Sydney, Sydney, Australia, in 1993.

He is currently a Professor of microphotonics and Director of the Electron Science Research Institute (ESRI) and the WA Centre of Excellence for MicroPhotonic Systems, Edith Cowan University, Joondalup, Australia. He is also a World-Class University (WCU) Professor with the Department of Nano-bio Materials and Electronics, Gwangju Institute of Science and Technology (GIST), Korea, Adjunct Professor with Glamorgan University, Wales, U.K., and Guest Professor with Southeast University, Nanjing, China. He has pioneered the integration of microelectronic and photonic sciences and developed a new and practical research area, "MicroPhotonics," and currently he is engaged in research and development on Opto-VLSI, optoelectronics, and micro-/nano-photonics targeting innovative solutions to fundamental issues in ICT, agriculture, health, consumer electronics, and security and defense. He has authored or coauthored over 200 peer-reviewed journal and conference papers, including three book chapters, and filed 21 patents.

Prof. Alameh is a member of a number of editorial boards of international journals and takes a senior role in the organization of conferences and other scientific events. He was the recipient of the WA Inventor of the Year (Early Stage) in 2007, the Inaugural Vice-Chancellor Award for Excellence in Research, Edith Cowan University, in 2008, and the Khalil Gibran International Award in 2010.